

# 1 **The mode of the climacogram estimator for a Gaussian Hurst-** 2 **Kolmogorov process**

3 Short Title: Same

4 Panayiotis Dimitriadis\* and Demetris Koutsoyiannis

5 Department of Water Resources and Environmental Engineering, School of Civil Engineering,  
6 National Technical University of Athens, Heroon Polytechneiou 5, 15880 Zographou, Greece

7 \*corresponding author, email: pandim@itia.ntua.gr

## 8 **Abstract**

9 Geophysical processes are often characterized by long-term persistence. An important  
10 characteristic of such behaviour is the induced large statistical bias, i.e. the deviation of a  
11 statistical characteristic from its theoretical value. Here, we examine the most probable value  
12 (i.e. mode) of the estimator of variance to adjust the model for statistical bias. Particularly, we  
13 conduct an extensive Monte-Carlo analysis based on the climacogram (i.e. variance of the  
14 average process vs. scale) of the simple scaling (Gaussian Hurst-Kolmogorov) process, and we  
15 show that its classical estimator is highly skewed especially in large scales. We observe that the  
16 mode of the climacogram estimator can be well approximated by its lower quartile (25%  
17 quartile). To derive an easy-to-fit empirical expression for the mode we assume that the  
18 climacogram estimator follows a gamma distribution, an assumption strictly valid for Gaussian  
19 white noise processes. The results suggest that when a single timeseries is available it is  
20 advantageous to estimate the Hurst parameter using the mode estimator rather than the  
21 expected one. Finally, it is discussed that while the proposed model for mode bias works well for  
22 Gaussian processes, for higher accuracy and non-Gaussian processes one should perform a  
23 Monte-Carlo simulation following an explicit generation algorithm.

24 **Keywords:** statistical bias, long-term persistence, stochastic uncertainty, mode estimator,  
25 climacogram

## 26 **1. Introduction**

27 An important attribute characterizing geophysical processes is the high spatio-temporal  
28 dependence, in the sense that a random variable of such a process at a specific time or location  
29 strongly depends on several (even infinite) past, or of different location, random variables of the  
30 same process. This type of dependence requires long samples for its identification, which is a  
31 rare case in most natural processes, and thus, for the estimation of its parameters it is advised to  
32 use only up to the second-order statistics (Lombardo et al., 2014) and only in cases where very  
33 long samples are available to expand to higher orders. The above issues are further highlighted  
34 in Dimitriadis (2017), where several (overall thirteen) such processes with various lengths and  
35 physical properties expanding from small-scale turbulence to large-scale hydrometeorological  
36 processes are analyzed in terms of their long-term behaviour using massive databases and  
37 unbiased estimators of the second-order dependence structure. Interestingly, all the examined  
38 processes exhibited long-term-persistence, else known as Hurst-Kolmogorov (HK) behaviour  
39 (coined by Koutsoyiannis and Cohn, 2008), i.e. power-law decay of the autocorrelation function  
40 with lag (for a literature review on long-term persistent processes in hydrometeorology see also

41 O'Connell et al., 2016). Additionally, Koutsoyiannis (2011) provided a theoretical justification of  
42 the HK behaviour in geophysical processes showing that it is linked to the second-law of  
43 thermodynamics (i.e. entropy extremization), and specifically, the stronger the persistence of  
44 the dependence structure of a process, the higher the entropy of the process at large scales.

45 The identification of the dependence structure of a process can be highly affected by the sample  
46 uncertainty and statistical bias, where the true statistical properties (mean, variance etc.) of a  
47 statistic (e.g. variance) of a stochastic process may differ from the one estimated from a series  
48 with finite length. The deviations of the statistical characteristics from their true values should  
49 be taken into account not only for the marginal characteristics but also for the dependence  
50 structure of the process. Therefore, to correctly adjust the stochastic model to the observed  
51 series of the physical process we should account for the bias effect since all series are of finite  
52 (and often short) lengths.

53 The second-order properties can be similarly assessed by common stochastic tools such as the  
54 autocovariance function (a function of lag), power spectrum (a function of frequency), and  
55 variation of statistics (e.g. variance) of the averaged process vs. scale, a tool known as  
56 climacogram (Koutsoyiannis, 2010). It is shown that the latter estimator of the second-order  
57 dependence structure, as compared to the other two metrics, encompasses additional  
58 advantages in stochastic model building and interpretation from data; for example, it is  
59 characterized by smaller statistical uncertainty and easier to handle expressions of the statistical  
60 bias (Dimitriadis and Koutsoyiannis, 2015). Therefore, it is advisable that the sample  
61 uncertainty of the second-order dependence structure be tackled with the estimator with the  
62 lower variation, such as the climacogram. When multiple sample realizations (i.e. recorded  
63 series) are known, the handling of the statistical bias arising from a selected stochastic model  
64 may be based on the unbiased estimator of the expected value of the climacogram (Dimitriadis  
65 and Koutsoyiannis, 2018). However, when a single data series of observations is available for the  
66 model fitting (which is the case when geophysical processes are studied), it would be interesting  
67 to examine the mode of the climacogram, instead of the expected value; the two may differ in  
68 case of strong HK behaviour. This estimator is equivalent to a maximum-likelihood estimator  
69 (e.g. Kendzioriski et al., 1999) for processes with zero (i.e. white noise) or short-term (e.g.  
70 Markov) dependence structure, while here we further extend it for HK processes (see also the  
71 work of Tyrallis and Koutsoyiannis, 2011, for the expectation of the climacogram). It is noted that  
72 while the climacogram is often based on the second central moment (i.e. variance) other types of  
73 moments (e.g. raw, L-moments or K-moments; Koutsoyiannis, 2019) can be used to measure  
74 fluctuation in scale, and here, we focus on the central second-order climacogram (i.e. fluctuation  
75 measured by variance vs. scale).

## 76 **2. Methods**

77 In this section we present the applied methods, namely the climacogram estimator, the  
78 statistical bias expressions for the mode and expected values of the estimator and the algorithm  
79 for the stochastic synthesis of the Gaussian HK process for the Monte-Carlo analysis.

### 80 **2.1. The climacogram**

81 The analysis of a process through the variance of the averaged process vs. scale has been  
82 thoroughly applied in stochastic processes (e.g. Papoulis 1991; Vanmarcke, 2010). However, its

83 importance to the analysis of the second-order dependence structure is highlighted mainly by  
 84 more recent works (see a historical review in Koutsoyiannis, 2018). Also, the simple name  
 85 *climacogram* allowed its further understanding through visualization; indeed, the term  
 86 originates from the Greek *climax* (meaning scale) and *gramma* (meaning written; cf. the terms  
 87 autocorrelogram for the autocorrelation, scaleogram for the power spectrum and wavelets).

88 It has been shown that the climacogram, treated as an estimator (rather than just a tool for the  
 89 identification of long-term behaviour of the second-order dependence structure), has additional  
 90 advantages from the more widely applied estimators of the autocovariance and power spectrum  
 91 (Dimitriadis and Koutsoyiannis, 2015). Namely, the climacogram could provide a more direct,  
 92 easy and accurate means to make diagnoses from data and build stochastic models in  
 93 comparison to the power spectrum and autocovariance. For example, the climacogram,  
 94 compared to other tools, has the lowest standardized estimation error for processes with short-  
 95 term and long-term persistence, zero discretization error for averaged processes, simple and  
 96 analytical expression for the statistical bias, always positive values, well defined and usually  
 97 monotonic behaviour, smallest fluctuation of skewness on small scales while closest to zero  
 98 skewness in larger scales, and mode closest to the expected (i.e. mean) value in large scales.  
 99 Also, the climacogram is directly linked to the entropy production of a process (Koutsoyiannis,  
 100 2011; 2016). Furthermore, the climacogram expands the notion of *variance* by making it a  
 101 function of *time scale* and is per se further expandable for statistics different from the central  
 102 estimators of fluctuation (e.g. second raw moment, second L-moment vs. scale; Koutsoyiannis,  
 103 2019), for different characteristics of the estimator (e.g. mode, median), and even for moments  
 104 of higher (e.g. third, fourth) orders (Dimitriadis and Koutsoyiannis, 2018). Recently,  
 105 Koutsoyiannis (2019) extended the notion of climacogram for orders higher than two and  
 106 showed how to substitute the joint moments of a process, allowing in this manner to tackle some  
 107 limitations of the latter such as the discretization effect and statistical bias.

108 Symbolically, the climacogram is:

$$\gamma(k) := \text{var}[\underline{x}(k)] \quad (1)$$

109 where  $\text{var}[\ ]$  denotes the variance and  $\underline{x}(k) := 1/k \int_0^k \underline{x}(t)dt$  is the continuous-time process at  
 110 scale  $k$  (in dimensions of time), which equals the discrete-one averaged in time intervals  $\Delta$ , i.e.  
 111  $\underline{x}_\kappa := 1/\kappa \sum_{i=1}^\kappa x_i$ , in the discrete-time scale  $\kappa=k/\Delta$  (dimensionless natural number whereas for  
 112 real numbers see adjustment in Koutsoyiannis, 2011).

## 113 2.2. The Gaussian long-term persistent process and its stochastic synthesis

114 The most common processes employed in geophysics, and particularly in hydrology, are the  
 115 white noise process, the Markov process (with an exponential decay of the autocorrelation) and  
 116 long-term persistent processes, which are characterized by a power-law decay of the  
 117 climacogram (or equivalently of the autocorrelation) as a function of scale (or lag). A typical  
 118 representative of the latter processes is the Gaussian HK process defined as:

$$(\underline{x}(k) - \mu) =_d (k)^{(H-1)} (\underline{x}(1) - \mu) \quad (2)$$

119 where  $=_d$  denotes equality in distribution with  $\mu$  the mean and  $\gamma(k) = \gamma(\Delta)/\kappa^{2-2H}$  the variance  
 120 of the process for each scale  $k$ ,  $H$  is the Hurst parameter ( $0 < H < 1$ ) else defined as (Dimitriadis

121 et al., 2016a)  $H := 1 + \frac{1}{2} \lim_{k \rightarrow \infty} d \ln(\gamma(k)) / d \ln k$ ; the quantity in the limit is the derivative of  
 122  $\ln(\gamma(k))$  with respect to  $\ln(k)$ .

123 It is noted that this process has infinite variance at scale zero and thus, it should not be used to  
 124 model the small scales of a physical process (in spite of the fact that the fractional-Gaussian-  
 125 noise -fGn- process is widely used to model several processes at small scales; Koutsoyiannis et  
 126 al., 2018). For the stochastic synthesis of the Gaussian HK model, we may use the sum of  
 127 arbitrarily many independent Markov processes, thus expressing the target climacogram as  
 128 (Dimitriadis and Koutsoyiannis, 2015):

$$\gamma(\kappa\Delta) = \sum_{i=1}^l \frac{2\lambda_i}{(\kappa\Delta/q_i)^2} (\kappa\Delta/q_i + e^{-\kappa\Delta/q_i} - 1) \quad (3)$$

129 where  $\lambda_i$  is the variance and  $q_i$  a time scale parameter for each Markov model  $i$ , and  $l$  the total  
 130 number of Markov processes. Mandelbrot (1963) has shown that for  $l \rightarrow \infty$  the above model can  
 131 adequately describe an fGn (or else Gaussian HK) process for any generated length (see also  
 132 Mandelbrot and Wallis, 1968; Mandelbrot and van Ness, 1968). Koutsoyiannis (2002) has  
 133 analytically estimated the parameters of three AR(1) models ( $l = 3$ ) to capture the HK process  
 134 for  $n < 10^4$ . Dimitriadis and Koutsoyiannis (2015) have expanded this framework to the sum of  
 135 arbitrarily many AR(1) models (abbreviated as SAR) for the generation of any type of process  
 136 with autoregressive dependence structure and up to any number of scales, by using a suitable  
 137 function with only two parameters, namely  $p_1$  and  $p_2$ , that link the lag-1 autocorrelations of each  
 138 Markov model, e.g. through the expression  $q_i = p_1 p_2^{i-1}$ , with  $i = 1, \dots, l$  and  $l$  often taken equal to  
 139 the integer part of  $\log(n)+1$ . For example, for  $n = 10^6$  and  $H = 0.8$ , we have  $l = 7$ ,  $p_1 = 0.394$  and  
 140  $p_2 = 12.356$  for a maximum standardized error between the true  $\gamma_t$  (Eqn. 2) and modelled  $\gamma_m$   
 141 (Eqn. 3) climacogram (i.e.  $\max|\gamma_t - \gamma_m| / \gamma_t$  for all scales) equal to 0.009 (Table 1).

142 Table 1: Parameters  $p_1$  and  $p_2$  estimated to approximate different types of the N(0,1)-HK model  
 143 (i.e.  $\mu = 0$  and  $\gamma(\Delta) = 1$ ) with  $l = 7$  and  $n \leq 10^6$ .

$H$	$p_1$	$p_2$	maximum error (standardized)
0.51	0.022	17.122	0.001
0.60	0.091	12.607	0.006
0.70	0.124	13.317	0.009
0.80	0.394	12.356	0.009
0.90	0.395	14.708	0.005
0.99	0.548	19.465	0.001

144

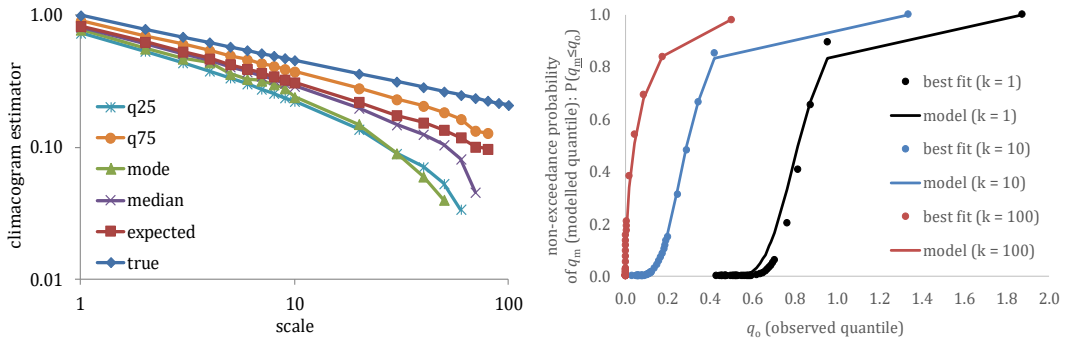
### 145 2.3. The mode of climacogram estimator and its statistical bias

146 The climacogram can be estimated from a sample through an estimator as similarly done for the  
 147 estimators of the marginal moments. Here, for the climacogram we use a classical estimator:

$$\hat{\gamma}(\kappa\Delta) = \frac{1}{[n/\kappa] - 1} \sum_{i=1}^{[n/\kappa]} \left( x_i^{(\kappa)} - \bar{x} \right)^2 \quad (4)$$

148 where  $[n/\kappa]$  is the integer part of  $n/\kappa$ ,  $x_i^{(\kappa)} = \sum_{l=\kappa(i-1)+1}^{\kappa i} x_l / \kappa$  is the averaged process at scale  
 149  $\kappa = k/\Delta$  for  $i \in [1, [n/\kappa]]$ ,  $\bar{x} = \sum_{l=1}^n x_l / n = x_{-1}^{(n)}$  is the sample average and  $n$  is the series length.

150 Since the above estimator is a random variable, it has a marginal distribution (see an illustration  
 151 in Fig. 1). The true value of a statistical characteristic (e.g. variance) of a stochastic model may  
 152 differ from the one estimated from a series with finite length. To correctly adjust the stochastic  
 153 model to the observed series of the physical process one should account for the bias effect. An  
 154 important question is how the statistical bias is generally handled through the second-order  
 155 dependence structure in case of long-term persistent processes. Particularly, the selected  
 156 stochastic model should be adjusted for bias before it is fitted to the sample dependence  
 157 structure. It is noted that neglecting the bias effect in case of a long-term persistent process  
 158 leads to underestimations of the stochastic model parameters such as the Hurst parameter, and  
 159 to erroneous conclusions. Adjustment of the models for bias is usually done by equating the  
 160 observed dependence structure to the expected value of the applied estimator. The alternative  
 161 studied here is the mode, instead of the expected value, of the dependence structure, which  
 162 represents the most probable value (and thus, the most expected) of the variance estimator at  
 163 each scale.



164 Figure 1: An illustration for a  $N(0,1)$ -HK ( $H = 0.83$ ,  $n = 200$ ) process of [left] how several  
 165 statistical characteristics of the climacogram estimator vary with scale and [right] the observed  
 166 quantile ( $q_o$ ) vs. the non-exceedance probability of the modelled quantile  $P(q_m \leq q_o)$ , showing how  
 167 the gamma distribution can adequately approximate the distribution of the climacogram  
 168 estimator especially at large scales.  
 169

170 The statistical bias of an estimator is the difference of the expected value of an estimator from its  
 171 true value (e.g. Papoulis, 1991). Thus, the bias of the climacogram is (e.g. Koutsoyiannis, 2011):

$$B_E [\hat{\gamma}(\kappa\Delta)] = E [\hat{\gamma}(\kappa\Delta)] - \gamma(\kappa\Delta) = \frac{(\kappa/n)\gamma(\kappa\Delta) - \gamma(n\Delta)}{1 - \kappa/n} \quad (5)$$

172 where  $B_E[\cdot]$  denotes the bias of the expected value of a statistical estimator of a process. Clearly,  
 173 for the mean value of a process we have that  $B_E [\hat{\mu}] = E[\sum_{l=1}^n x_l / n] - \mu = 0$ .

174 Following the same rationale, we define an expansion of the notion of bias for the mode of the  
 175 above estimator of the climacogram, i.e.:

$$B_M[\hat{\gamma}(\kappa\Delta)] = M[\hat{\gamma}(\kappa\Delta)] - \gamma(\kappa\Delta) \quad (6)$$

176 where  $M[\underline{x}] := \arg \max[f(\underline{x})]$  denotes the mode of the variable  $\underline{x}$  with density function  $f(x)$ . We  
 177 refer to  $B_M[\ ]$  as the mode bias.

178 For a Gaussian white noise process of length  $n$  and variance  $\gamma(1)$  the distribution of its sample  
 179 variance follows the gamma distribution  $\Gamma((n-1)/2, 2\gamma(1)/(n-1))$  (Cochran, 1934). The  
 180 averaged process at scale  $\kappa$ , with sample length of  $n/\kappa$  and variance  $\gamma(k) = \gamma(\Delta)/\kappa$ , follows  
 181  $\Gamma((n/\kappa-1)/2, 2\gamma(\Delta)/(n-\kappa))$ , with  $M[\hat{\gamma}(\kappa\Delta)] = \gamma(\Delta) \frac{n-3\kappa}{\kappa(n-\kappa)}$  for  $n/\kappa \geq 3$ , else 0. Hence, for  
 182  $n/\kappa \gg 3$  we have that  $(n-3\kappa)/(n-\kappa) \approx 1$ , and  $M[\hat{\gamma}(\kappa\Delta)] \approx E[\hat{\gamma}(\kappa\Delta)] = \gamma(\Delta)/\kappa = \gamma(\kappa\Delta)$ , i.e.  
 183 zero bias. However, for long-term persistent processes the mode bias is non-zero and its  
 184 analytical solution is no longer possible.

185 From the above results it becomes evident that the statistical bias always depends on the  
 186 selected model and not on the data as commonly thought. For example, consider the Gaussian-  
 187 HK process in the previous section with an autocorrelation function in discrete-time  
 188  $\rho_v = 1/2(|v+1|^{2H} + |v-1|^{2H}) - |v|^{2H}$ , where  $v$  is the discrete-time lag. The bias of the  
 189 autocorrelation is similarly defined as  $B_E[\hat{\rho}(v)] = E[\hat{\rho}(v)] - \rho(v)$ , and thus, depends on the  
 190 model parameter  $H$ . It is noted that the above apply even to the so-called non-parametric  
 191 models, since they also involve estimation from data, and thus, these models should be similarly  
 192 adjusted for statistical bias to avoid underestimation of the process variability during a Monte-  
 193 Carlo simulation.

194 For simplicity, and without loss of generality, we set  $\Delta = 1$  for the rest of the analysis. It is evident  
 195 that  $B_M[\hat{\gamma}(\kappa)] \leq B_E[\hat{\gamma}(\kappa)] \leq 0$  or else  $|B_E[\hat{\gamma}(\kappa)]| \leq |B_M[\hat{\gamma}(\kappa)]|$ , since the sample variance is  
 196 positively skewed, i.e.  $E[\hat{\gamma}(\kappa)] \geq M[\hat{\gamma}(\kappa)]$ , and the equality holds when  $n \rightarrow \infty$ , where the  
 197 variance of the sample variance is zero for an ergodic process. A preliminary analysis of common  
 198 HK-type processes has shown that the mode climacogram is close to the low quartile (25%  
 199 quantile) of the marginal distribution of variance at each scale (Dimitriadis et al., 2016c;  
 200 Gournary, 2017). Therefore, when the mode of the variance estimator is of interest, we may use  
 201 a Monte-Carlo technique (as described in the next section) to accurately estimate the mode bias  
 202 or, in case the marginal distribution of the climacogram is known, to calculate the 25% quantile  
 203 at each scale to approximate the mode bias.

### 204 3. Monte-Carlo analysis for the mode of the variance estimator

205 We perform Monte-Carlo experiments over the N(0,1)-HK model for a wide range of Hurst  
 206 parameters  $H$  (i.e. 0.5 to 0.95), and for a wide range of series lengths  $n$  (i.e. 20 to 2000).  
 207 Specifically, we produce a number ( $N$ ) of synthetic series through the SAR model described in  
 208 section 2.2, where  $N$  depends on the sample mean value to reach the expected one at scale  $\kappa =$   
 209  $n/10$  based on the rule of thumb when using the climacogram as shown in Dimitriadis and  
 210 Koutsoyiannis (2015). We found that for  $N \approx 10^6/n^{2-2H}$  the standardized error between the  
 211 theoretical expected value and the sample one (Eqn. 5) is lower than 1% at scale  $\kappa = n/10$ . In this  
 212 way, the mode is expected also to be well preserved with a similar error. However, caution  
 213 should be given to the selection of the sample mode estimator to ensure that its variance permits  
 214 a robust estimation of the true value of the mode. Since the distribution function of the estimator



215 of variance is unknown for long-term persistent processes, and given that the mode value is the  
 216 most probable to occur within the sample, we calculate the sample mode from each simulated  
 217 series by finding the most probable value with an accuracy of two decimal digits. Specifically, we  
 218 round up each value of the time series, and for each scale, to the second decimal digit, and we  
 219 estimate the most probable value of the rounded time series (for higher accuracies a larger  $N$   
 220 was required). Also, other estimators for the sample mode (e.g. Bickel and Fruwirth, 2006) could  
 221 be used and compared to the proposed one in future research to optimize the performance of  
 222 the analysis.

223 Here, to derive an easy-to-fit empirical expression to approximate the mode bias, we adopt the  
 224 assumption that the above distribution is nearly gamma for smaller scales (see also a similar  
 225 analysis in Gournary, 2017, and Dimitriadis et al., 2018). Using the results from the Monte-Carlo  
 226 analysis we then evaluate the parameter of the gamma distribution for each  $H$ ,  $n$  and  $\kappa$ , and we  
 227 build a model for the mode, which we later test its performance. Although the true  
 228 autocorrelation function of the averaged process for a long-term persistent process does not  
 229 vary with scale, the sample autocorrelation will be also prone to bias (e.g. Dimitriadis and  
 230 Koutsoyiannis, 2015) affecting the distribution function of the sample variance at each scale. To  
 231 minimize the sample error for the fitting of the two-parameter gamma distribution we use the  
 232 theoretical expression for the expected value of the sample climacogram, i.e.  $E[\hat{\gamma}(\kappa)]$ , and the  
 233 variance of the sample climacogram, i.e.  $\text{Var}[\hat{\gamma}(\kappa)]$ , as evaluated from the Monte-Carlo analysis,  
 234 which exhibits the lowest variability in estimation among the four central moments (Dimitriadis  
 235 and Koutsoyiannis, 2018, Fig. 2). Based on these two measures, we estimate the two parameters  
 236 of the gamma distribution.

237 We first set the scale parameter of the gamma distribution such as to simulate the sample ratio  
 238 of the aforementioned parameters, i.e.  $b(H, n, \kappa) = \text{Var}[\hat{\gamma}(\kappa)]/E[\hat{\gamma}(\kappa)]$  and so, the shape  
 239 parameter can be also estimated as  $a(H, n, \kappa) = E[\hat{\gamma}(\kappa)]/b(H, n, \kappa)$ .

240 We observe (e.g. Fig. 2) that for  $a(H, n, \kappa) > 1$  the shape parameter  $a(H, n, \kappa)$  is approximately  
 241 proportional, by a function  $c(H)$ , to the corresponding shape parameter for the white noise  
 242 process  $a(0.5, n, \kappa) = (n/\kappa - 1)/2$  raised to a function  $p(H)$ , i.e.:

$$a(H, n, \kappa) = c(H) \left( (n/\kappa - 1)/2 \right)^{p(H)} \quad (7)$$

243 where  $a(H, n, \kappa) > 1$  is a function corresponding to the shape parameter of the gamma  
 244 distribution function, while for  $a(H, n, \kappa) \leq 1$  or  $\kappa \gtrsim n/3$ , the mode is considered close to zero.

245 The two functions of the above expression are fitted as (Fig. 2):

$$c(H) = 1.68(H - 0.5)^2 - 0.3025(H - 0.5) + 1 \quad (8)$$

246 and

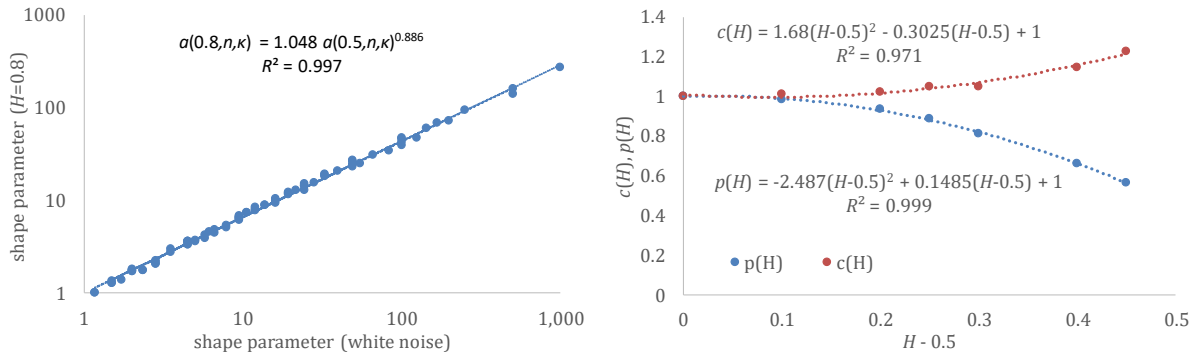
$$p(H) = -2.4865(H - 0.5)^2 + 0.1485(H - 0.5) + 1 \quad (9)$$

247 The above two adjustments allow to empirically express the mode of the climacogram estimator  
 248 as a function of  $H$ ,  $n$  and  $\kappa$ :

$$M[\hat{\gamma}(\kappa)] = (a(H, n, \kappa) - 1)b(H, n, \kappa) = (1 - 1/a(H, n, \kappa))E[\hat{\gamma}(\kappa)] \quad (10)$$

249 It is noted that based on the above assumptions the standard deviation, and the skewness and  
 250 excess kurtosis coefficients of the climacogram estimator can be estimated as  
 251  $b(H, n, \kappa)\sqrt{a(H, n, \kappa)}$ ,  $2/\sqrt{a(H, n, \kappa)}$ , and  $6/a(H, n, \kappa)$ , respectively. Since  $a(H, n, \kappa) \leq a(0.5, n, \kappa)$   
 252 all the above measures will be larger than those in case of a white noise process.

253 The above expression can approximate the mode by an absolute difference of 0.005 from the  
 254 Monte-Carlo estimates, while for better approximations it is advised to implement a new Monte-  
 255 Carlo analysis (see also discussion and application in sect. 4). Interestingly, the standardized  
 256 error between the mode and expected values of the estimator, i.e.  $\varepsilon = |E[\hat{\gamma}(\kappa)] - M[\hat{\gamma}(\kappa)]| /$   
 257  $E[\hat{\gamma}(\kappa)]$ , is calculated from the Monte-Carlo analysis to reach a maximum value of 67%  
 258 corresponding to cases with  $H \geq 0.6$  and  $n/\kappa \leq 10$ , while for the white noise process it can be  
 259 theoretically estimated as  $\varepsilon = 2/(n/\kappa - 1)$ , which for  $\kappa = n/10$  is approximately 20%.

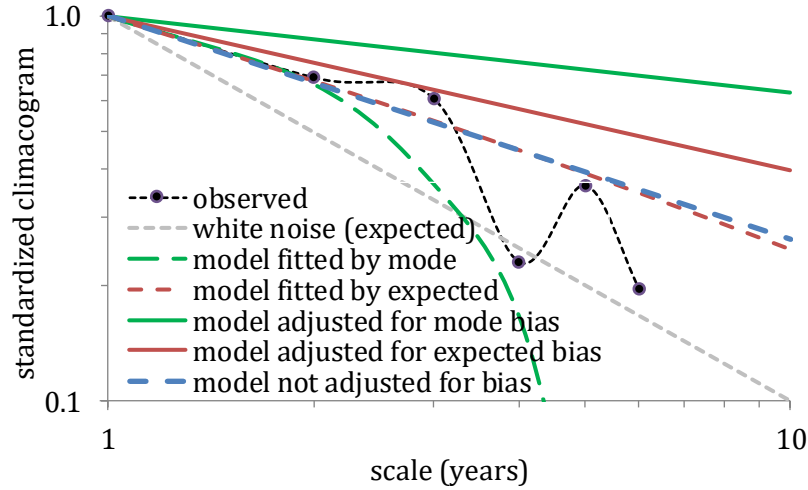


260  
 261 Figure 2: [left] The shape parameter assuming a gamma distribution for the mode estimator of  
 262 the climacogram of an  $N(0,1)$ -HK process (for  $H = 0.8$  and for all  $n$  and  $\kappa$  simulated in the Monte-  
 263 Carlo analysis) versus the theoretical shape parameter of the white noise process. [right]  
 264 Proposed model for the  $c(H)$  and  $p(H)$  functions for all examined  $H$  from the Monte-Carlo  
 265 analysis.

## 266 4. Applications to annual streamflow

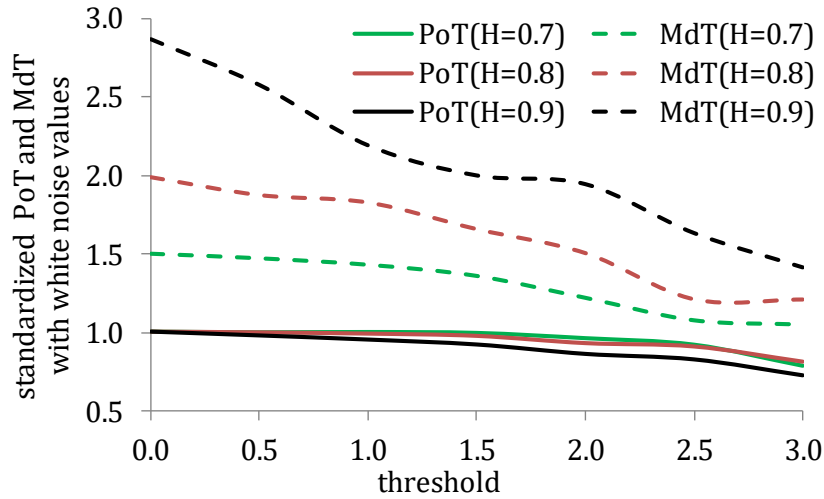
267 For illustrations of possible implications of the above results, we apply a stochastic analysis  
 268 based on the expected and the mode values of the climacogram to a streamflow process at the  
 269 Peneios river (Thessaly, Greece), where a historical streamflow annual time series is available at  
 270 the upstream station of Ali Efenti with only a 13 years length (for more information on the study  
 271 area see Dimitriadis et al., 2016b). For the identification of the stochastic model we adjust for  
 272 statistical bias and, in particular, we fit the mode of the estimator rather than its expectation. It  
 273 is noted that the proposed empirical model for the mode bias (Eqn. 10) is derived from a Monte-  
 274 Carlo analysis for sample lengths of  $n \geq 20$ , and so for this application we perform a new Monte-  
 275 Carlo analysis to fit the observed climacogram for scales  $1 \leq \kappa \leq n/10$  (rule of thumb; Dimitriadis  
 276 and Koutsoyiannis, 2015) and so here, for the first two scales (Fig. 3). We find that an HK model  
 277 can adequately simulate the observed standardized climacogram, i.e.  $\hat{\gamma}(\kappa)/\hat{\gamma}(1)$ , with  $H = 0.9$ .  
 278 We also estimate the Hurst parameter with the expectation of the estimator, and we find  $H' \approx 0.8$   
 279 and  $H'' \approx 0.7$ , with or without adjusting for bias, respectively. Evidently, both latter values  
 280 underestimate the long-term persistence behaviour (Fig. 3).





281  
 282 Figure 3: Standardized climacogram estimations of the observed standardized time series (black  
 283 line), the white noise model (grey line), and the three fitted  $N(0,1)$ -HK stochastic processes: (a)  
 284 adjusting for bias of the mode of the estimator (green line), i.e.  $M[\hat{\gamma}(\kappa)]/M[\hat{\gamma}(1)]$ , , and of its  
 285 expectation (red line), i.e.  $E[\hat{\gamma}(\kappa)]/E[\hat{\gamma}(1)]$ , and (b) not adjusting for bias (blue line), i.e.  
 286  $\hat{\gamma}(\kappa) = \gamma(\kappa)$ , also corresponding to the non-parametric model configuration.

287 It is noted that the dependence structure of a process (e.g. streamflow) will have a small effect at  
 288 the risk imposed by the expected number of peaks over threshold (e.g. for the design of a dam or  
 289 for flood risk mapping) as compared to the effect of the marginal distribution of the process  
 290 (Volpi et al., 2015; Serinaldi and Kilsby, 2018). However, the dependence structure will have a  
 291 great effect (especially for processes with long-term behaviour) at the duration of successive  
 292 peaks over threshold (e.g. maximum duration of wet/dry periods or of flood inundation), which  
 293 may highly affect urban as well as agricultural areas and insurance policies (e.g. Serinaldi and  
 294 Kilsby, 2016; Goulianou et al., 2019). To illustrate this, we generate an adequate number  $N$  (see  
 295 sect. 3) of HK synthetic timeseries with  $H = 0.5$  ( $N = 5 \times 10^3$ ),  $H = 0.7$  ( $N = 4 \times 10^4$ ),  $H = 0.8$  ( $N = 10^5$ )  
 296 and  $H = 0.9$  ( $N = 3 \times 10^5$ ). For convenience and simplification, we assume a  $N(0,1)$  distribution for  
 297 all processes. We then estimate the expected frequency of the number of peaks over various  
 298 thresholds (PoT) as well as the expected frequency of the maximum duration of successive  
 299 peaks over various thresholds (MdT), and we standardize them with the PoT and MdT values of  
 300 the white noise process (Fig. 4). We find that the MdT varies with threshold and long-term  
 301 persistence while the PoT stays almost unaffected by both. Additional analyses and  
 302 quantifications on the reflection of long-term term persistence in terms of clustering in time can  
 303 be found in Iliopoulou and Koutsoyiannis (2019).



304

305 Figure 4: Expected frequency of peak over threshold (PoT) and expected maximum duration of  
 306 successive peaks over threshold (MdT) standardized with the PoT and MdT values of the  $N(0,1)$   
 307 white noise process for various HK- $N(0,1)$  processes.

308 The results from this study suggest that the sample estimator of the variance can be skewed  
 309 even for long samples in the presence of long-term persistence behaviour as opposed to the  
 310 white noise process. Therefore, the mode is different from the expectation and more suitable to  
 311 use in estimation. We propose that, when a single recorded series is available and a Gaussian HK  
 312 process is fitted with small sample size and relatively high Hurst parameter, it is advantageous  
 313 to employ the mode of the estimator as calculated from the empirical model of Eqn. 10, rather  
 314 than its expectation (Eqn. 5), so as to avoid underestimation of the Hurst parameter (and thus,  
 315 the uncertainty of the process). In case of a non-Gaussian distribution, larger accuracy or a  
 316 different estimator of the second-order dependence structure (e.g. other climacogram estimator,  
 317 autocovariance, power spectrum, variogram etc.), we should employ the Monte-Carlo technique  
 318 and test whether the mode of the estimator used is close enough to its expected value. If this is  
 319 true then the expected value can be used to adjust the model for bias, whereas if the two values  
 320 vary then for the model should be adjusted for bias based on the mode estimator. For Monte-  
 321 Carlo analysis of a non-Gaussian correlated process an explicit algorithm should be preferred  
 322 (Dimitriadis and Koutsoyiannis, 2018) since the mode value is expected to highly depend on  
 323 higher-order moments in case of long-term persistent processes.

## 324 5. Conclusions and discussion

325 Awareness of uncertainty in assessing the dependence structure of a process is of paramount  
 326 importance as it may critically affect the interpretation of results. Estimation uncertainty may  
 327 introduce large statistical bias, which can be additionally magnified in the presence of long-term  
 328 persistence (Dimitriadis and Koutsoyiannis, 2015). In addition, if the uncertainty is  
 329 underestimated then a regular cluster of events could be erroneously regarded as an extreme  
 330 cluster. Although the mode of the examined classical estimator for variance is close to its  
 331 expectation for small Hurst parameters and large lengths, we show that for larger values of the  
 332 Hurst parameter and small sample lengths, equating the expected climacogram to the observed  
 333 one may lead to underestimation of the long-term persistence and thus, the uncertainty of the  
 334 process.

335 We propose that when the available series have short lengths or when the empirical Hurst  
336 parameter is estimated larger than 0.5, we should always account for statistical bias. Particularly  
337 for the bias adaptation, when information is available on only a single series/realization of the  
338 process, it is advantageous to equate the mode instead of the expectation of the climacogram  
339 estimator to the sample values. Interestingly, in case of a  $N(0,1)$ -HK process, the absolute  
340 difference between the mode and expected values of the estimator is calculated (from a Monte-  
341 Carlo analysis performed in this study) to reach a maximum value of 67% of the expected value,  
342 corresponding to cases with  $H \geq 0.6$  and  $n/\kappa \leq 10$ , while for the white noise process is  
343 approximately 20% for  $\kappa = n/10$ . In cases of different stochastic processes or estimators or  
344 when a larger accuracy of the mode bias is of interest, one should employ a Monte-Carlo  
345 technique through an explicit generation algorithm (Dimitriadis and Koutsoyiannis, 2018) to  
346 estimate the mode climacogram estimator or use the lower quartile (25% quantile) of the  
347 estimator (in case its distribution is known) as an approximation.

348 From the Monte-Carlo analysis performed in this study, it is also observed that for a  $N(0,1)$ -HK  
349 process with variance  $\gamma(\kappa) = \gamma(1)/\kappa^{2-2H}$ , and for large  $n$  and small  $n/\kappa$ , the distribution of the  
350 climacogram estimator tends to that of  $\Gamma((n/\kappa - 1)/2, 2\gamma(\kappa)/(n/\kappa - 1))$ , with a mean value of  
351  $\gamma(\kappa)$ , i.e. zero bias. However, given the estimation uncertainty present in records exhibiting  
352 persistence, the autocorrelation of the averaged process is independent of the scale, and thus,  
353 the above distribution will never be truly reached. The underestimation of the persistence of the  
354 parent process has also critical implications for the estimation of the properties of its extremes,  
355 as it was shown that the maximum duration of successive peaks over threshold is greatly  
356 affected by the degree of dependence. Additional analyses and quantifications on the reflection  
357 of long-term term persistence in terms of clustering in time can be found in Iliopoulou and  
358 Koutsoyiannis (2019).

359 A final remark for discussion, considering the etymology of the terms, is that the expected value  
360 of a random process is less expected to occur than its mode (i.e. most probable value; a term  
361 coined by Pearson, 1895, p. 345), where only in symmetrical distributions the two coincide.  
362 Therefore, when only one value is known (here, only one realization of the climacogram  
363 estimator), it is more accurate to fit the model and evaluate the Hurst parameter based on the  
364 proposed mode estimator rather than the expected one.

## 365 **Acknowledgment**

366 The Authors would like to thank the Editor Luigi Berardi for handling the paper, one anonymous  
367 Reviewer for useful comments, and Federico Lombardo for his fruitful discussion, comments and  
368 suggestions that helped us improve the paper.

## 369 **Code availability**

370 The MATLAB script for the SAR generation algorithm is available as well as the script for a fast  
371 estimation algorithm of the sample climacogram in very long timeseries and in many scales.

## 372 **References**

373 Bickel, D.R. and Fruwirth, R., On a fast, robust estimator of the mode: Comparisons to other  
374 robust estimators with applications, *Computational Statistics & Data Analysis*, 50: 3500–3530,  
375 2006.

376 Cochran, W. G., The distribution of quadratic forms in a normal system, with applications to the  
377 analysis of covariance, *Mathematical Proceedings of the Cambridge Philosophical Society*, 30 (2):  
378 178–191. doi:10.1017/S0305004100016595, 1934.

379 Dimitriadis, P., Hurst-Kolmogorov dynamics in hydrometeorological processes and in the  
380 microscale of turbulence, PhD thesis, 167 pages, *National Technical University of Athens*, 2017.

381 Dimitriadis, P., and D. Koutsoyiannis, Climacogram versus autocovariance and power spectrum  
382 in stochastic modelling for Markovian and Hurst–Kolmogorov processes, *Stochastic  
383 Environmental Research & Risk Assessment*, 29 (6), 1649–1669, 2015.

384 Dimitriadis, P., and D. Koutsoyiannis, Stochastic synthesis approximating any process  
385 dependence and distribution, *Stochastic Environmental Research & Risk Assessment*, 32 (6),  
386 1493–1515, doi:10.1007/s00477-018-1540-2, 2018.

387 Dimitriadis, P., D. Koutsoyiannis, and P. Papanicolaou, Stochastic similarities between the  
388 microscale of turbulence and hydrometeorological processes, *Hydrological Sciences Journal*, 61  
389 (9), 1623–1640, doi:10.1080/02626667.2015.1085988, 2016a.

390 Dimitriadis, P., A. Tegos, A. Oikonomou, V. Pagana, A. Koukouvinos, N. Mamassis, D.  
391 Koutsoyiannis, and A. Efstratiadis, Comparative evaluation of 1D and quasi-2D hydraulic models  
392 based on benchmark and real-world applications for uncertainty assessment in flood mapping,  
393 *Journal of Hydrology*, 534, 478–492, 2016b.

394 Dimitriadis, P., N. Gournari, and D. Koutsoyiannis, Markov vs. Hurst-Kolmogorov behaviour  
395 identification in hydroclimatic processes, *European Geosciences Union General Assembly*, Vol. 18,  
396 EGU2016-14577-4, 2016c.

397 Dimitriadis, P., N. Gournary, A. Petsiou and D. Koutsoyiannis, How to adjust the fGn stochastic  
398 model for statistical bias when handling a single time series; application to annual flood  
399 inundation, *13th Hydroinformatics Conference*, 1-6 July 2018, Palermo, Italy, 2018.

400 Goulianou, T., K. Papoulakos, T. Iliopoulou, P. Dimitriadis, and D. Koutsoyiannis, Stochastic  
401 characteristics of flood impacts for agricultural insurance practices, *European Geosciences Union  
402 General Assembly*, Vol. 21, EGU2019-5891, 2019.

403 Gournary, N., *Probability distribution of the climacogram using Monte Carlo techniques*, Diploma  
404 thesis, 108 pages, Department of Water Resources and Environmental Engineering – National  
405 Technical University of Athens, Athens, July 2017 (in Greek).

406 Iliopoulou, T., and D. Koutsoyiannis, Revealing hidden persistence in maximum rainfall records,  
407 *Hydrological Sciences Journal*, doi.org/10.1080/02626667.2019.1657578, 2019.

408 Koutsoyiannis, D., The Hurst phenomenon and fractional Gaussian noise made easy,  
409 *Hydrological Sciences Journal*, 47 (4), 573–595, 2002.

410 Koutsoyiannis, D., HESS opinions “A random walk on water”, *Hydrology and Earth System  
411 Sciences*, 14, 585–601, 2010.

412 Koutsoyiannis, D., Hurst-Kolmogorov dynamics as a result of extremal entropy production,  
413 *Physica A: Statistical Mechanics and its Applications*, 390 (8), 1424–1432, 2011.

414 Koutsoyiannis, D., Generic and parsimonious stochastic modelling for hydrology and beyond,  
415 *Hydrological Sciences Journal*, 61 (2), 225–244, 2016.

416 Koutsoyiannis, D., Climate change impacts on hydrological science: A comment on the  
417 relationship of the climacogram with Allan variance and variogram, *ResearchGate*, 2018.

418 Koutsoyiannis, D., Knowable moments for high-order stochastic characterization and modelling  
419 of hydrological processes, *Hydrological Sciences Journal*, 2019.

420 Koutsoyiannis, D., and T.A. Cohn, The Hurst phenomenon and climate (solicited), *European*  
421 *Geosciences Union General Assembly*, Vol. 10, Vienna, 11804, doi:10.13140/RG.2.2.13303.01447,  
422 European Geosciences Union, 2008.

423 Koutsoyiannis, D., Dimitriadis, P., Lombardo, F., and Stevens, S., *From fractals to stochastic:*  
424 *Seeking theoretical consistency in analysis of geophysical data*, Advances in Nonlinear  
425 Geosciences, edited by A.A. Tsonis, 237–278, Springer, 2018.

426 Kendzioriski, C.M., J.B. Basingthwaighte, and P.J. Tonellato, Evaluating maximum likelihood  
427 estimation methods to determine the Hurst coefficient, *Physica A*, V. 273, 3-4, pp. 439–451, 1999.

428 Lombardo, F., E. Volpi, D. Koutsoyiannis, and S.M. Papalexiou, Just two moments! A cautionary  
429 note against use of high-order moments in multifractal models in hydrology, *Hydrology and*  
430 *Earth System Sciences*, 18, 243–255, doi:10.5194/hess-18-243-2014, 2014.

431 Mandelbrot, B.B., The Variation of Certain Speculative Prices, *J. Bus.*, 36, 394–419, 1963.

432 Mandelbrot, B.B. and Wallis, J.R., Noah, Joseph and operational hydrology, *Water Resour. Res.*, 4,  
433 909–918, 1968.

434 Mandelbrot, B.B., and Van Ness, J.W., Fractional Brownian Motions, Fractional Noises and  
435 Applications, *SIAM Rev.*, 10, 422–437, 1968.

436 O’Connell P.E., D. Koutsoyiannis, H. F. Lins, Y. Markonis, A. Montanari, and T.A. Cohn, The  
437 scientific legacy of Harold Edwin Hurst (1880 – 1978), *Hydrological Sciences Journal*, 61 (9),  
438 1571–1590, doi:10.1080/02626667.2015.1125998, 2016.

439 Papoulis, A., Probability, *Random Variables and Stochastic Processes*, 3rd edn., McGraw-Hill, New  
440 York, 1991.

441 Pearson, K., Contributions to the mathematical theory of evolution—II, Skew variation in  
442 homogeneous material, *Philosophical Transactions of the Royal Society of London*, 186, 343-  
443 414, 1895 (available at <https://royalsocietypublishing.org/doi/pdf/10.1098/rsta.1895.0010>).

444 Serinaldi, F., and Kilsby, C.G., Understanding Persistence to Avoid Underestimation of Collective  
445 Flood Risk. *Water*, 8, 152, 2016.

446 Serinaldi, F., and Kilsby, C.G., Unsurprising Surprises: The Frequency of Record-breaking and  
447 Over-threshold Hydrological Extremes Under Spatial and Temporal Dependence, *Water*  
448 *Resources Research*, 54(9), 6460-6487, 2018.

449 Tyralis, H., and D. Koutsoyiannis, Simultaneous estimation of the parameters of the Hurst-  
450 Kolmogorov stochastic process, *Stochastic Environmental Research & Risk Assessment*, 25 (1),  
451 21–33, 2011.

452 Vanmarcke, E., *Random Fields: Analysis and Synthesis*, World Scientific, New Jersey, USA, 2010.

453 Volpi, E., Fiori, A., Grimaldi, S., Lombardo, F., and Koutsoyiannis, D., One hundred years of return  
454 period: Strengths and limitations, *Water Resources Research*, 51(10), 8570-8585, 2015.